



QUANTIFYING RAINFALL - EVAPOTRANSPIRATION IMBALANCE AND IRRIGATION WATER DEFICIT IN THE BANTIMURUNG IRRIGATION AREA, MAROS, INDONESIA

Abd Rakhim Nanda

Universitas Muhammadiyah Makassar, Indonesia

*Email: abd.rakhimnanda@unismuh.ac.id

Abstract

This study quantifies irrigation water deficit in the Bantimurung Irrigation District (Maros, Indonesia) by integrating rainfall-evapotranspiration imbalance into a hydrological-agronomic water balance. Monthly rainfall (CHIRPS) and reference evapotranspiration (Open-Meteo) for 2000–2024 were combined with crop coefficients and a local planting calendar to estimate effective rainfall and net irrigation requirement (NIR). Despite cumulative rainfall of 81,077.6 mm exceeding crop evapotranspiration (34,450.6 mm; 2.35:1), deficits occurred in 96 of 300 months (32%), concentrated in July–October. Total NIR was ~9,044 mm ($\approx 361.8 \text{ mm yr}^{-1}$), with 97.35% accruing in the dry season and peak demand in August–September. The maximum monthly deficit was 200.93 mm (September 2023) and the most severe year was 2015 (711.12 mm).

Keywords: water balance, effective rainfall, crop evapotranspiration, net irrigation requirement, dry-season deficit

INTRODUCTION

The resilience of agricultural production in irrigated areas is determined by water availability at the operational scale (monthly to seasonal), not solely by annual rainfall surpluses (Perez et al., 2024; Wang et al., 2024). Within a hydrological-agronomic framework, the evaluation of water sufficiency must be based on a water balance that links rainfall, the portion that is truly effective for crops (effective rainfall/ P_{eff}), and crop evapotranspiration requirements (ET_c) derived from reference evapotranspiration (ET_0), crop coefficients, and the planting calendar (da Silva et al., 2024; Xing et al., 2024; Zhang et al., 2024). Because only a portion of rainfall becomes available water (influenced by runoff, percolation, and the mismatch between rainfall timing and growth phases), high-rainfall areas can still experience deficits when P_{eff} lags ET_c during peak demand periods (Villani et al., 2024).

This paradox was observed in the Bantimurung Irrigation District, Maros. During 2000–2024, cumulative rainfall (81,077.6 mm) exceeded ET_0 (34,450.6 mm; a ratio of 2.35:1), yet an irrigation deficit still occurred in 96 out of 300 months (32.0%), primarily from July to October, with a maximum deficit of approximately 201 mm (September 2023). This pattern confirms that the climatological surplus cannot be treated as a proxy for crop water sufficiency, as the primary determinant is the temporal mismatch between P_{eff} and ET_c during the dry season when evapotranspiration demand increases.

Given these conditions, this study developed a hydrological-agronomic water balance framework to quantify the rainfall-evapotranspiration imbalance and translate it into operational irrigation deficit indicators at monthly, seasonal, and

interannual scales (Kayatz et al., 2024; Pronti et al., 2024). The gap addressed is the lack of long-term, location-based evaluations that consistently integrate rainfall, $\frac{ET_0}{ET_c}$, P_{eff} , net irrigation requirements, and cropping season dynamics into measures of deficit (magnitude, frequency, intensity, severity, and critical windows). The contribution of this research is the quantitative demonstration that rainfall surpluses are not equivalent to irrigation sufficiency, as well as the provision of an analytical basis for irrigation scheduling, water allocation priorities during July-October, and crop calendar adjustments to reduce the risk of water stress during critical growth phases (Bao et al., 2024; Teshome et al., 2023).

METHOD

Figure 1 presents an analytical framework that links hydroclimatic inputs (P, ET_0) and agronomic parameters (cropping calendar, K_c) to estimates of P_{eff} , ET_c , net irrigation requirement (NIR), and deficit diagnostics across various timescales (Hezam et al., 2024).

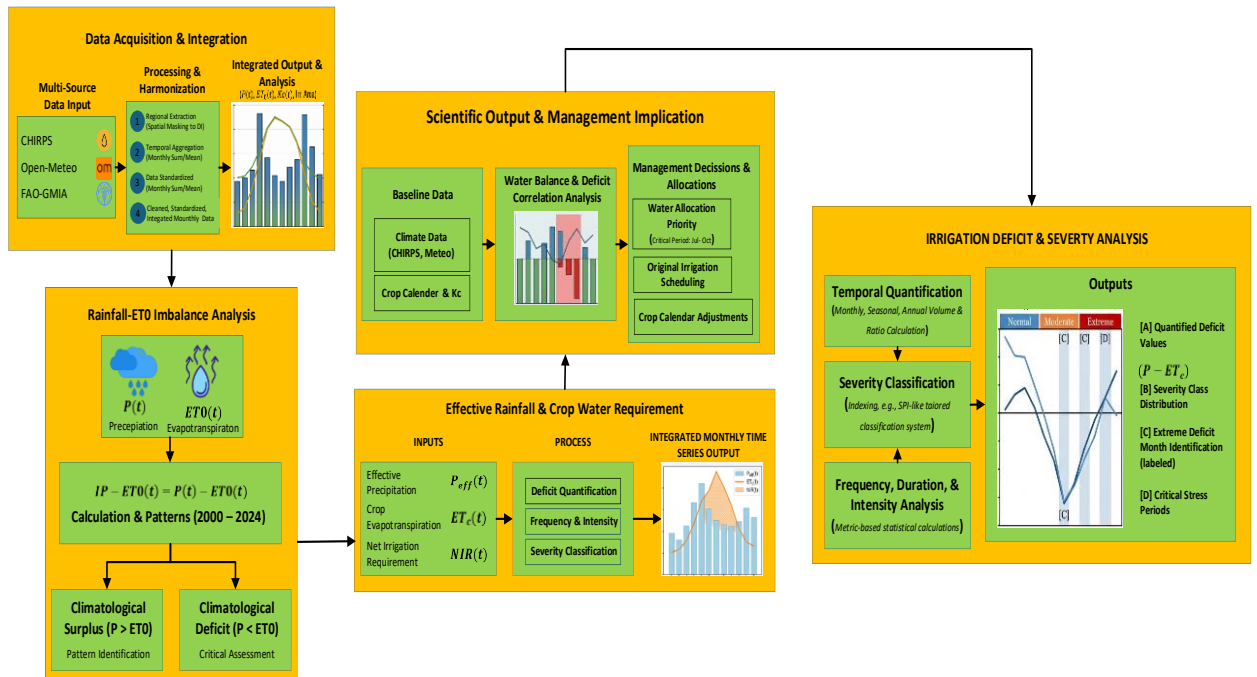


Figure 1. Deficit Analysis Workflow

The study was conducted in the Bantimurung Irrigation District, Maros, Indonesia, using monthly data from 2000 to 2024. The analysis procedure included harmonization of rainfall data (CHIRPS) and ET_0 (Open-Meteo), parameterization of the cropping calendar and crop coefficient (K_c), estimation of effective rainfall (P_{eff}), and calculation of crop water requirements ($ET_c = K_c \cdot ET_0$) (Abou Ali et al., 2023; Mekonnen et al., 2024). Net irrigation requirements are calculated as:

$$NIR = \max(0, ET_c - P_{eff})$$

This used to derive deficit indicators on monthly, seasonal, and annual scales (magnitude, frequency, intensity, accumulation, and extreme events) to

identify the primary risk window (July–October) and support operational interpretation . The data are shown in Table 1.

Table 1. Data inputs and roles

Data Components	Source/unit	Analytical role
Rainfall (P)	CHIRPS; mm/bulan	Climatological balance inputs (P_{ET0}) and effective rainfall base
Mold evapotranspiration ($ET0$)	Open-Meteo; mm/bulan	Atmospheric and input demand proxies ET_c
Service limits/areas	FAO GMIA; ha/spatial boundaries	Conversion of deficit depth to volume and territorial context
Planting calendar	Local sources; Phase/month	Timing parameterization ET_c
Plant coefficients (Kc)	Literature; Ununited	Convert $ET0$ to ET_c . ($ET_c = Kc \cdot ET0$)

Indicators are calculated monthly and aggregated seasonally/annually, Deficits are classified low-medium-weight based on distribution to mark critical periods (Kuang et al., 2024). If the service area is available, the depth deficit (mm) is converted to volume (m^2).

$$I_{P-ET0}(t) = P(t) - ET0(t)$$

with $P(t)$ and $ET0(t)$ represent precipitation and reference evapotranspiration in month t ; $I_{P-ET0}(t) > 0$ indicates a climatological surplus, while < 0 indicates atmospheric pressure exceeding precipitation input. To ensure the interpretability of the transition from the climatic context to irrigation pressure, the diagnostic indicators used are summarized in Table 2.

Table 2. Diagnostic indicators

Indicators	Analytical objectives
$P - ET0$	Diagnosis of climatological surplus/deficit
$P/ET0$	Context of rainfall dominance vs. atmospheric demand
$\frac{P_{eff}}{ET_c}$	Test of effective rainfall sufficiency relative to crop needs
NIR	Estimation of net irrigation requirement ($\max(0, ET_c - P_{eff})$)
Deficit (mm)	Magnitude, frequency, intensity, accumulation, and critical periods

These indicators are then used to report deficits across different time scales and, when necessary, to convert deficit depth into volume so that the data is relevant for water allocation operations(Dong et al., 2024). The conversion from depth (mm) to volume (m^3) is necessary to relate the magnitude of the deficit to supply capacity and distribution needs within the service area.

$$V_{def} = D_{def} \times A \times 10$$

$V_{def} (m^3)$ is the volume deficit, D (mm) is the depth of the deficit, and A (ha) is the service area. Volume calculations are performed only when service area data is available and consistent with the boundaries of the analysis area.

RESULT AND DISCUSSIONS

Climate Balance Diagnostics

On a climatological scale, Bantimurung exhibits a significant water surplus: during 2000-2024, cumulative rainfall (81,077.6 mm) exceeded ET_0 (34,450.6 mm; a ratio of 2.35:1). However, this metric only indicates the dominance of aggregate rainfall input and is insufficient to conclude on the adequacy of irrigation water, as crop needs and irrigation services are determined by seasonal dynamics, effective rainfall, and peak evapotranspiration demand. As shown in Figure 2.

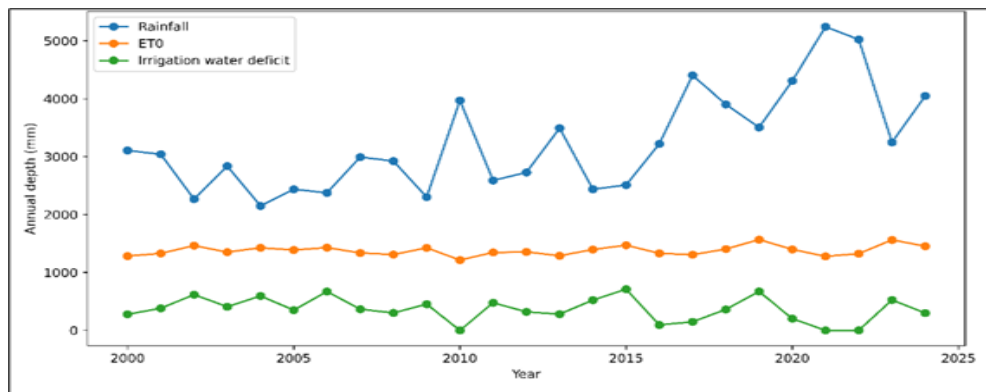


Figure 2. Annual rainfall vs ET0 (2000-2024)

When broken down into monthly resolutions, this annual surplus reveals a temporal mismatch: rainfall is concentrated in December-March, while ET_0 increases in August-October when rainfall is at its lowest. The July-September period is when ET_0 approaches or exceeds rainfall, making the climatological surplus no longer a relevant indicator of irrigation water availability during this critical operational window. As shown in Figure 3.

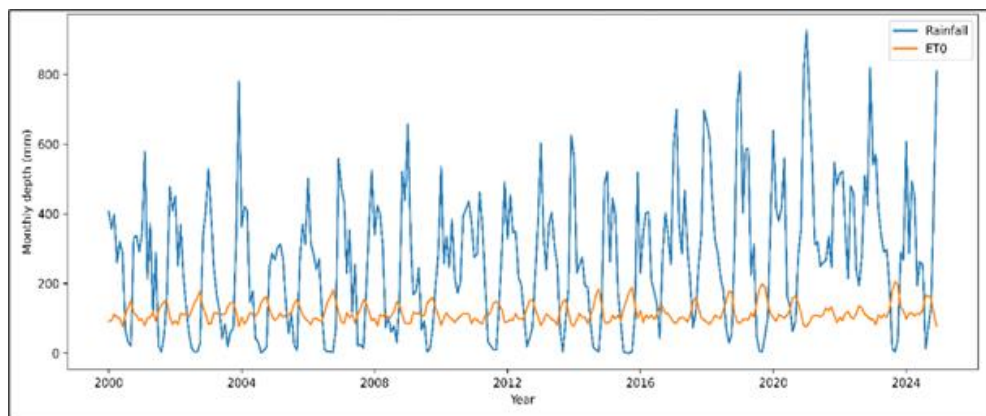


Figure 3. Mean monthly rainfall vs ET0 (2000-2024)

Effective rainfall adequacy

Compared to total rainfall, effective rainfall (P_{eff}) is a more diagnostic indicator of crop water availability because it represents the portion of rainfall that can actually be utilized. Aggregately (2000-2024), cumulative P_{eff} (37,176.5 mm) is slightly higher than crop evapotranspiration (ET_c ; 34,450.6 mm), but this

aggregate sufficiency is illusory because its distribution does not align with the calendar of water needs.

During the rainy season (January-March and December), P_{eff} generally exceeds ET_c , whereas during the dry season, P_{eff} drops sharply as ET_c increases. The most critical conditions occur in August-September, when P_{eff} is only about 38.46-46.86 mm/month, while ET_c reaches about 141.77-155.18 mm/month. Thus, the deficit is primarily driven by the mismatch between P_{eff} and ET_c during high-demand months, rather than by an annual rainfall shortfall. As shown in Figure 4.

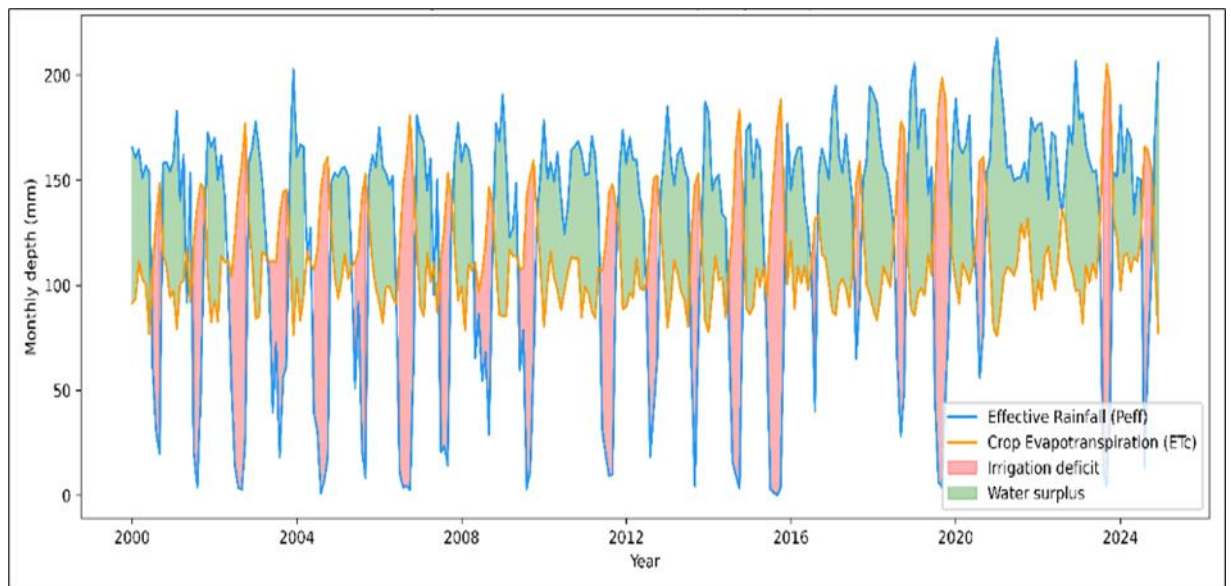


Figure 4. Mean monthly P_{eff} vs ET_c (2000-2024)

Irrigation demand (NIR)

The imbalance between P_{eff} and ET_c has a direct impact on net irrigation requirements (NIR). During 2000-2024, the cumulative NIR reached approximately 9,044 mm (an average of approximately 361.8 mm/year), representing the additional water supply required when effective rainfall does not cover crop evapotranspiration needs. NIR is highly seasonal and concentrated between July and October, with peak averages in September (113.5 mm/month) and August (105.4 mm/month). Seasonally, the dry season accounts for 97.35% of total NIR (8,804.1 mm), while the rainy season accounts for only 2.65% (239.9 mm). This dominance confirms that the main challenge for irrigation services in Bantimurung is the reliability of supply during the dry season, rather than annual water availability. The result is presented in Figure 5.

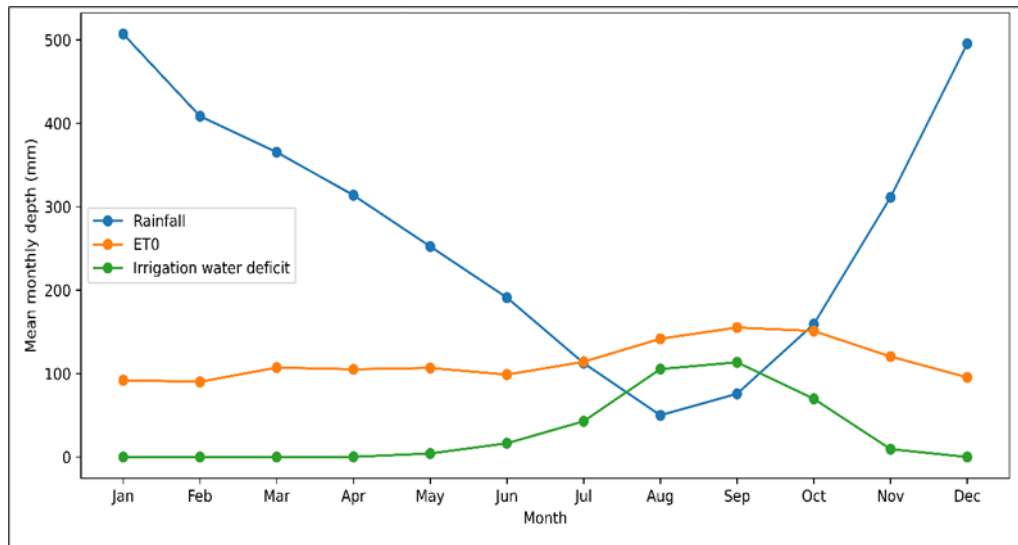


Figure 5. Mean monthly NIR and deficit signals (2000-2024)

Deficit regime and extremes

Over the 2000–2024 period, irrigation deficits occurred in 96 out of 300 months (32.0%), with a cumulative total of 9,044 mm. This figure confirms that a climatological rainfall surplus does not equate to sufficient irrigation service, as deficits form during combinations of months with low P_{eff} and high evapotranspiration demand. Temporally, the deficit is concentrated in July-October, peaking in August-September the period when the $P_{eff}-ET_c$ gap is at its maximum. The average intensity during deficit months reaches 94.21 mm, meaning that each instance of a deficit has direct implications for water distribution scheduling and prioritization. The result is presented in Figure 5.

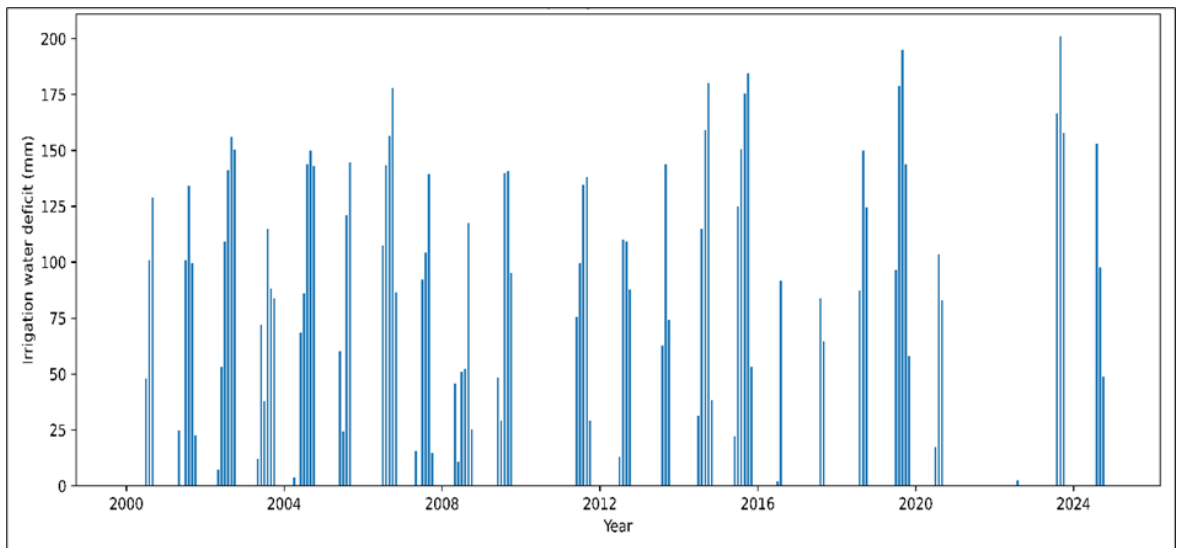


Figure 6. Monthly irrigation deficit series (2000-2024)

Extremes highlight interannual variability: the maximum deficit was recorded in September 2023 (200.93 mm), while 2015 recorded the highest annual deficit (711.12 mm). In contrast, 2010 and 2021 showed no deficit, indicating that

irrigation risk is shaped by interannual climate variability rather than merely average seasonal patterns.

Table 3. Top 5 monthly deficits

Period	P (mm)	ET0 (mm)	Deficit (mm)
2023-09	4.3	205.2	200.9296
2019-09	3.9	198.87	194.9943
2015-10	3.7	188.35	184.6719
2014-10	3.4	183.45	180.0685

Decision relevance and limitations

From a management perspective, these results identify July-October as the key decision window: during this phase, P_{eff} is consistently insufficient, $\frac{ET_0}{ET_c}$ increases, and NIR/deficit reaches its peak. The practical implication is risk-based irrigation scheduling, namely prioritizing supply in August-September, aligning water distribution with high-demand growth phases, and considering adjustments to the planting calendar so that critical phases do not coincide with the peak of the deficit. The findings also suggest that evaluations of irrigation service reliability should emphasize temporal metrics (frequency, intensity, and extreme events) rather than relying solely on annual surplus indicators.

Table 4. Seasonal deficit summary 2000-2024

Season	P (mm)	ET0 (mm)	Deficit (mm)	Contribution (%)
Dry season	21.032,40	19.190,26	8.804,12	97,35
Rainy season	60.045,20	15.260,29	239,87	2,65

The seasonal summary shows that the deficit is almost entirely concentrated in the dry season (97.35% of the total). Mechanistically, this concentration is consistent with a mismatch between P_{eff} and ET_c during dry months when evapotranspiration demand increases, meaning that the annual climatological surplus does not alleviate irrigation pressure during the operational window. The main limitation of this study lies in the use of grid datasets and empirical estimates of P_{eff} , meaning spatial uncertainties (heterogeneity in rainfall, soil, and distribution losses) as well as network operational factors (channel efficiency, actual flow rates, and distribution rules) are not fully accounted for. Therefore, the results are best interpreted as a diagnosis of deficits at the service area scale; enhanced field validation (channel flow, irrigation supply, soil moisture) is recommended to improve alignment with operational conditions.

CONCLUSSIONS

This study shows that a water surplus on a climatological scale is not synonymous with sufficient irrigation on an operational scale. In Bantimurung (2000-2024), the ratio of rainfall to ET_0 is approximately 2.35:1, yet an irrigation deficit still occurs in 32.0% of the observation months and is concentrated in July-October. The primary mechanism is a temporal mismatch between effective rainfall (P_{eff}) and crop evapotranspiration (ET_c) during the dry season, which increases net irrigation requirements and triggers extreme events (peak in September 2023; most stressed year in 2015).



Scientifically, the hydrological-agronomic water balance framework based on $P-ET_0$, $P_{eff}-ET_c$, and deficit indicators provides a quantitative diagnosis for irrigation scheduling, water allocation priorities, and adjustments to the planting calendar during critical windows. Future research should focus on higher-resolution hydro-meteorological data, the integration of actual evapotranspiration based on remote sensing and soil moisture observations, and the inclusion of network operation parameters (efficiency, distribution losses, flow/supply) so that results are better calibrated to actual service conditions and can be extended to prospective evaluations based on climate change scenarios.

REFERENCES

1. Abou Ali, A., Bouchaou, L., Er-Raki, S., Hssaissoune, M., Brouziyne, Y., Ezzahar, J., Khabba, S., Chakir, A., Labbaci, A., & Chehbouni, A. (2023). Assessment of crop evapotranspiration and deep percolation in a commercial irrigated citrus orchard under semi-arid climate: Combined Eddy-Covariance measurement and soil water balance-based approach. *Agricultural Water Management*, 275, 107997. <https://doi.org/10.1016/j.agwat.2022.107997>
2. Bao, X., Zhang, B., Dai, M., Liu, X., Ren, J., Gu, L., & Zhen, W. (2024). Improvement of grain weight and crop water productivity in winter wheat by light and frequent irrigation based on crop evapotranspiration. *Agricultural Water Management*, 301, 108922. <https://doi.org/10.1016/j.agwat.2024.108922>
3. da Silva, I. W. H., Marques, T. V., Urbano, S. A., Mendes, K. R., Oliveira, A. C. C. F., Nascimento, F. da S., de Moraes, L. F., Pereira, W. dos S., Mutti, P. R., Emerenciano Neto, J. V., Lima, J. R. de S., Oliveira, P. E. S., Costa, G. B., Santos e Silva, C. M., & Bezerra, B. G. (2024). Meteorological and biophysical controls of evapotranspiration in tropical grazed pasture under rainfed conditions. *Agricultural Water Management*, 299, 108884. <https://doi.org/10.1016/j.agwat.2024.108884>
4. Dong, H., Dong, J., Sun, S., Bai, T., Zhao, D., Yin, Y., Shen, X., Wang, Y., Zhang, Z., & Wang, Y. (2024). Crop water stress detection based on UAV remote sensing systems. *Agricultural Water Management*, 303, 109059. <https://doi.org/10.1016/j.agwat.2024.109059>
5. Hezam, I. M., Ali, A. M., Sallam, K., Hameed, I. A., & Abdel-Basset, M. (2024). An efficient decision-making model for evaluating irrigation systems under uncertainty: Toward integrated approaches to sustainability. *Agricultural Water Management*, 303, 109034. <https://doi.org/10.1016/j.agwat.2024.109034>
6. Kayatz, B., Baroni, G., Hillier, J., Lüdtkke, S., Freese, D., & Wattenbach, M. (2024). Supporting decision-making in agricultural water management under data scarcity using global datasets – chances, limits and potential improvements. *Agricultural Water Management*, 296, 108803. <https://doi.org/10.1016/j.agwat.2024.108803>
7. Kuang, N., Hao, C., Liu, D., Maimaitiming, M., Xiaokaitijiang, K., Zhou, Y., & Li, Y. (2024). Modeling of cotton yield responses to different irrigation

- strategies in Southern Xinjiang Region, China. *Agricultural Water Management*, 303, 109018. <https://doi.org/10.1016/j.agwat.2024.109018>
8. Mekonnen, Y. G., Alamirew, T., Malede, D. A., Pareeth, S., Bantider, A., & Chukalla, A. D. (2024). Tailoring the surface energy balance algorithm for land-improved (SEBALI) model using high-resolution land/use land cover for monitoring actual evapotranspiration. *Agricultural Water Management*, 303, 109058. <https://doi.org/10.1016/j.agwat.2024.109058>
 9. Perez, G., Coon, E. T., Rathore, S. S., & Le, P. V. V. (2024). Advancing process-based flood frequency analysis for assessing flood hazard and population flood exposure. *Journal of Hydrology*, 639, 131620. <https://doi.org/10.1016/j.jhydrol.2024.131620>
 10. Pronti, A., Auci, S., & Berbel, J. (2024). Water conservation and saving technologies for irrigation. A structured literature review of econometric studies on the determinants of adoption. *Agricultural Water Management*, 299, 108838. <https://doi.org/10.1016/j.agwat.2024.108838>
 11. Teshome, F. T., Bayabil, H. K., Schaffer, B., Ampatzidis, Y., Hoogenboom, G., & Singh, A. (2023). Exploring deficit irrigation as a water conservation strategy: Insights from field experiments and model simulation. *Agricultural Water Management*, 289, 108490. <https://doi.org/10.1016/j.agwat.2023.108490>
 12. Villani, L., Castelli, G., Yimer, E. A., Chawanda, C. J., Nkwasa, A., Van Schaeybroeck, B., Penna, D., van Griensven, A., & Bresci, E. (2024). Impacts of climate change and vegetation response on future aridity in a Mediterranean catchment. *Agricultural Water Management*, 299, 108878. <https://doi.org/10.1016/j.agwat.2024.108878>
 13. Wang, X., Cheng, Y., Liu, L., Niu, Q., & Huang, G. (2024). Improved understanding of how irrigated area expansion enhances precipitation recycling by land–atmosphere coupling. *Agricultural Water Management*, 299, 108904. <https://doi.org/10.1016/j.agwat.2024.108904>
 14. Xing, L., Cui, N., Liu, C., Guo, L., Zhao, L., Wu, Z., Jiang, X., Wen, S., Zhao, L., & Gong, D. (2024). Estimating daily kiwifruit evapotranspiration under regulated deficit irrigation strategy using optimized surface resistance based model. *Agricultural Water Management*, 295, 108745. <https://doi.org/10.1016/j.agwat.2024.108745>
 15. Zhang, Y., Zhu, G., Che, T., Wang, S., Xu, C., Chen, H., Zhang, Y., Su, Y., & Fan, H. (2024). The ratio of transpiration to evapotranspiration and water use efficiency in an irrigated oasis agroecosystem: Different temporal-scale effects. *Agricultural Water Management*, 302, 108980. <https://doi.org/10.1016/j.agwat.2024.108980>